The Astrophysical Journal Letters, 798:L19 (5pp), 2015 January 1 doi:10.1088/2041-8205/798/1/L19

ON THE ACCRETION-FED GROWTH OF NEUTRON STARS DURING COMMON ENVELOPE

Morgan MacLeod and Enrico Ramirez-Ruiz
Department of Astronomy and Astrophysics, University of California, Santa Cruz, CA 95064, USA
Received 2014 October 20; accepted 2014 December 3; published 2014 December 18

ABSTRACT

This paper models the orbital inspiral of a neutron star (NS) through the envelope of its giant-branch companion during a common envelope (CE) episode. These CE episodes are necessary to produce close pairs of NSs that can inspiral and merge due to gravitational wave losses in less than a Hubble time. Because cooling by neutrinos can be very efficient, NSs have been predicted to accumulate significant mass during CE events, perhaps enough to lead them to collapse to black holes. We revisit this conclusion with the additional consideration of CE structure, particularly density gradients across the embedded NS's accretion radius. This work is informed by our recent numerical simulations that find that the presence of a density gradient strongly limits accretion by imposing a net angular momentum to the flow around the NS. Our calculations suggest that NSs should survive CE encounters. They accrete only modest amounts of envelope material, $\lesssim 0.1\ M_\odot$, which is broadly consistent with mass determinations of double NS binaries. With less mass gain, NSs must spiral deeper to eject their CE, leading to a potential increase in mergers. The survival of NSs in CE events has implications for the formation mechanism of observed double NS binaries, as well as for predicted rates of NS binary gravitational wave inspirals and their electromagnetic counterparts.

Key words: accretion, accretion disks – binaries: close – stars: black holes – stars: evolution – stars: neutron

1. INTRODUCTION

The existence of a population of compact neutron star (NS) binaries (Hulse & Taylor 1975) serves as a unique probe of general relativity (Stairs 2004) and of binary stellar evolution (Bethe & Brown 1998; Kalogera et al. 2007; Postnov & Yungelson 2014). Mergers of NS binaries are promising sources for the detection of gravitational radiation (Phinney 1991; Belczynski et al. 2002), and are the progenitors of short gamma-ray bursts (Narayan et al. 1992; Behroozi et al. 2014). Yet, to inspiral and merge under the influence of gravitational radiation in less than a Hubble time, a compact binary must be separated by less than the radii of its main sequence progenitors (e.g., Peters 1964). To reach their current small separations, these binaries must have passed through one or more common envelope (CE) phases (Paczynski 1976).

In a standard evolutionary scenario to produce NS binaries, the companion to a NS evolves and engulfs the NS inside its growing envelope (Taam et al. 1978; Terman et al. 1995; Tauris & van den Heuvel 2006). Within the shared envelope, the NS focusses envelope gas toward itself. Flow convergence leads to dissipation of orbital energy in shocks and to accretion (Hoyle & Lyttleton 1939; Iben & Livio 1993; Ivanova et al. 2013). Neutrinos serve as an effective cooling channel for this convergent flow, allowing material to be incorporated into the NS at a hypercritical accretion rate well above the classical Eddington limit (Houck & Chevalier 1991; Fryer et al. 1996; Popham et al. 1999; Brown et al. 2000; Narayan et al. 2001; Lee et al. 2005; Lee & Ramirez-Ruiz 2006). The relative rates of drag and accretion implied by Hoyle & Lyttleton (1939) accretion (HLA) theory suggest that an inspiralling NS is likely to grow to collapse to a black hole (BH) before the CE is ejected (Chevalier 1993; Armitage & Livio 2000; Bethe et al. 2007), leaving behind a tightened remnant binary (Webbink 1984).

Despite this apparently clear prediction, reconciling the observed distribution of NS masses (e.g., Schwab et al. 2010; Özel et al. 2012; Kiziltan et al. 2013) with theories of hypercritical accretion in CE has posed a long-standing problem. In particular, double NSs exhibit a narrow range of inferred masses close to the suspected NS birth mass, centered at 1.33 $M_\odot$ with dispersion of 0.05 $M_\odot$ (Özel et al. 2012). Alternative evolutionary scenarios have been proposed where the NS can avoid CE and accretion entirely. For example, if the binary is sufficiently equal in mass, it could undergo a simultaneous, or *double core*, CE (Brown 1995). The issue is that for each binary that passed through a preferred channel one would expect numerous massive NS and BH-NS binaries assembled through the more standard channels (Fryer & Woosley 1998; Belczynski et al. 2002; Kalogera et al. 2007; Belczynski et al. 2010; Fryer et al. 2013). This picture remains at odds with the apparent paucity of BHs just above the maximum NS mass (Özel et al. 2010, 2012).

In this Letter, we re-evaluate claims that BHs should necessarily form via accretion-induced collapse during CE events involving a NS and its massive companion. We draw on results of our recent simulations of accretion flows within a stellar envelope to demonstrate that it is critical to consider not just the binding energy, but also the structural properties of the whole envelope (MacLeod & Ramirez-Ruiz 2014). To this end, we follow the inspiral and accretion of a NS during its dynamical inspiral and show that all NSs should be expected to survive CE evolution, accreting only a small fraction of their own mass.

2. CHARACTERISTIC CONDITIONS IN NS ACCRETION

When a NS becomes embedded within a CE, it exerts a gravitational influence on its surroundings and can accrete envelope material. In this section, we explore some characteristic scales for that accretion flow, focusing on how they depend on the supply of material and the microphysics of the gas.

2.1. Hoyle–Lyttleton Accretion within a CE

The flow around the NS can be described in the context of the NS's gravitational interaction with the surrounding medium in HLA theory (Hoyle & Lyttleton 1939). The NS's velocity relative to the envelope gas, v_∞, is typically mildly supersonic, $\mathcal{M}_\infty = v_\infty / c_{s,\infty} \gtrsim 1$, where $\mathcal{M}_\infty$ is the flow Mach number and

$c_{s,\infty}$ is the local sound speed. Material with an impact parameter less than an accretion radius,

$$R_a = \frac{2GM_{NS}}{v_\infty^2}, \quad (1)$$

is focused toward the NS. The resulting accretion rate is

$$\dot{M}_{HL} = \pi R_a^2 \rho_\infty v_\infty, \quad (2)$$

where ρ_∞ is the upstream density (Hoyle & Lyttleton 1939). Flow convergence leads to shocks that imply a rate of dissipation of kinetic energy, or *drag luminosity*,

$$\dot{E}_{HL} = \pi R_a^2 \rho_\infty v_\infty^3 = \dot{M}_{HL} v_\infty^2, \quad (3)$$

or a drag force of $F_{d,HL} = \dot{E}_{HL}/v_\infty$ (e.g., Iben & Livio 1993).

To estimate the growth of the NS during the inspiral, we first approximate the inspiral timescale as

$$t_{insp} \approx \frac{E_{orb}}{\dot{E}_{HL}}, \quad (4)$$

where $E_{orb} = GM_{NS}m/2a$ and m is the enclosed companion mass at a given orbital separation, a. The accreted mass is thus $\dot{M}_{HL} t_{insp}$, or

$$\Delta M_{NS} \sim \dot{M}_{HL} \frac{E_{orb}}{\dot{E}_{HL}} \sim \frac{M_{NS} m}{2(M_{NS}+m)}, \quad (5)$$

where we further assume that $v_\infty^2 = G(M_{NS}+m)/a$ in the second equality. This estimate reproduces, at the simplest level, the arguments of Chevalier (1993) and later Brown (1995) and Bethe & Brown (1998), who argue that the NS should grow substantially during its inspiral.

2.2. Microphysics and Hypercritical Accretion

The microphysics of accreting gas imposes several further scales on the accretion rate. The first of these is the Eddington limit. When the accretion luminosity reaches $L_{Edd} = 4\pi G M_{NS} c/\kappa$, where κ is the opacity, radiation pressure counteracts gravity and halts the accretion flow. This limit on the accretion luminosity implies a limit on the accretion rate,

$$\dot{M}_{Edd} \approx 2\times10^{-8} \left(\frac{R_{NS}}{12\ \mathrm{km}}\right) \left(\frac{\kappa}{0.34\ \mathrm{cm^2\ g^{-1}}}\right)^{-1} M_\odot\ \mathrm{yr}^{-1}. \quad (6)$$

The Eddington limit may be exceeded under certain conditions if photons are trapped in the accreting flow and carried inward. Photons are trapped within the flow within a trapping radius of approximately (Houck & Chevalier 1991),

$$R_{tr} = \frac{\dot{M}\kappa}{4\pi c} \approx 5.8\times10^{13} \left(\frac{\dot{M}}{M_\odot\ \mathrm{yr}^{-1}}\right) \left(\frac{\kappa}{0.34\ \mathrm{cm^2\ g^{-1}}}\right) \mathrm{cm}. \quad (7)$$

Because the NS has a surface, at small radii an accretion shock forms to stall the infalling gas. Within this shock neutrinos are the dominant cooling channel. The shock radius is

$$R_{sh} \approx 1.6\times10^{8} \left(\frac{\dot{M}}{M_\odot\ \mathrm{yr}^{-1}}\right)^{-0.37} \mathrm{cm}, \quad (8)$$

where the scaling with accretion rate arises from the neutrino cooling function (Houck & Chevalier 1991). When $R_{tr} > R_{sh}$, accretion energy is advected into the neutrino-cooling layer and super-Eddington, or hypercritical, accretion can proceed (Houck & Chevalier 1991). This implies a lower-limit accretion rate of

$$\dot{M}_{hyper} \approx 1.9\times10^{-4} \left(\frac{\kappa}{0.34\ \mathrm{cm^2\ g^{-1}}}\right)^{-0.73} M_\odot\ \mathrm{yr}^{-1}, \quad (9)$$

where if $\dot{M} \gtrsim \dot{M}_{hyper} \sim 10^4 \dot{M}_{Edd}$ accretion can proceed despite the violation of the photon Eddington limit. No cooling solutions exist for $\dot{M}_{Edd} < \dot{M} < \dot{M}_{hyper}$, so mass supplied at these rates can only be incorporated at $\dot{M}_{Edd}$.

Further investigation of these basic claims came in the form of multidimensional simulations, which confirmed that hypercritical accretion can reach a steady-state for some range of accretion rates while at others high entropy plumes intermittently overturn the flow (Fryer et al. 1996). For a flow with some rotational support, the critical $\dot{M}_{hyper}$ may be somewhat higher than for the spherical case described above (Chevalier 1996; Brown et al. 2000).

2.3. Limits on the Accretion Rate due to Flow Asymmetry

In order to track accretion onto a NS during CE, we need a clear prediction of the accretion rate as a function of CE structure. In MacLeod & Ramirez-Ruiz (2014), we use the FLASH adaptive mesh hydrodynamics code (Fryxell et al. 2000) to extend three-dimensional (3D) simulations of HLA to consider the role of an inhomogeneous upstream medium. We characterize the density gradient across the accretion radius as

$$\epsilon_\rho = \frac{R_a}{H_\rho}, \quad (10)$$

where $H_\rho = -\rho dr/d\rho$, the density scale height. A planar density gradient is then applied along the simulation y-axis, perpendicular to the direction of motion, with $\rho = \rho_\infty \exp(\epsilon_\rho y)$, where ρ_∞ is the density at zero impact parameter, $y = 0$. We find that typical values for ϵ_ρ in CE range from $\epsilon_\rho \approx 0.3$–3.

Strong density gradients break the symmetry that defines HLA, severely limiting accretion. The momenta of opposing streamlines do not fully cancel with the introduction of inhomogeneity, and the resulting flow carries angular momentum with respect to the accretor. Thus, even if material is gravitationally captured it may not be accreted because of this angular momentum barrier. The HLA formula, Equation (2), drastically overestimates the resultant accretion rate (see also Ricker & Taam 2008, 2012). In Figure 1, we show how flow morphology, drag force, and accretion rate change with steepening density gradients.

3. INSPIRAL AND ACCRETION

In order to trace the NS inspiral through the dynamical phase of CE evolution, we integrate coupled equations for the evolution of the orbit and accretion onto the NS. We discuss our initial models, evolution equations, and findings below.

3.1. Methods

To create approximate CE conditions, we evolve single stars in the MESA stellar evolution code (version 5527: Paxton et al. 2011, 2013). During the giant-branch phase, a CE event may be initiated when the radius of the stellar envelope grows to be similar to the binary separation, $R_* \sim a$. We make the simplifying approximation of a static CE profile. This is most

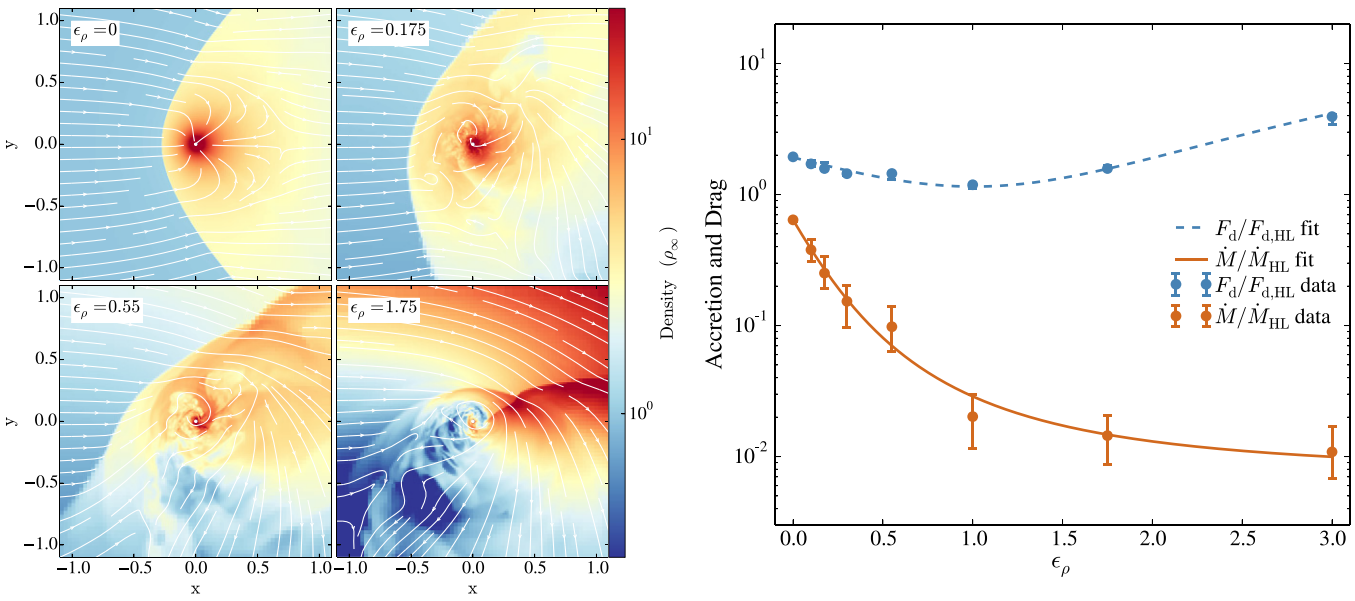

Figure 1. Flow morphologies, drag, and accretion in 3D simulations of HLA with an upstream density gradient. The introduction of upstream density gradients, as found in CE evolution, breaks the symmetry of HLA and gives rise to the tilted bow shock structures seen here. The coordinates in the flow panel are in units of the accretion radius, $R_{\rm a}$, and the accretor is defined as an absorbing sink condition with $R_{\rm s} = 0.01\ R_{\rm a}$ surrounding a central point mass. Flow momenta do not cancel in the wake of the accretor with upstream inhomogeniety and the post-shock region is defined by rotation. In the right panel, we compare the resultant drag and accretion rate normalized to values anticipated by HLA. We find that the drag force depends only mildly on density gradient, but the accretion rate decreases drastically as the density gradient, ϵ_ρ, steepens. These calculations use a gamma-law equation of state with $\gamma = 5/3$.

valid when the companion mass is much greater than the NS mass, $M_{\rm comp} \gg M_{\rm NS}$. The progenitors of NSs in binaries are massive stars, so we calculate the structure of giant-branch envelopes of with initial masses of 12–20 $M_\odot$. A comparison of these envelope structures, and the typical flow Mach numbers and density gradients they give rise to, is shown in Figure 2.

Orbital energy is dissipated at a rate

$$\dot{E}_{\rm orb} = -F_{\rm d}(\epsilon_\rho) v_\infty, \tag{11}$$

where $F_{\rm d}(\epsilon_\rho)$ is approximated using a fit to our simulation results described in Section 2.3,

$$\frac{F_{\rm d}(\epsilon_\rho)}{F_{\rm d,HL}} \approx f_1 + f_2\epsilon_\rho + f_3\epsilon_\rho^2, \tag{12}$$

with $f_i = (1.91791946,\ -1.52814698,\ 0.75992092)$. As a result of this drag, the orbital separation evolves at a rate $\dot{a} = \dot{E}_{\rm orb}(da/dE_{\rm orb})$. We terminate our integration of the dynamical inspiral when the integrated change in orbital energy equals the envelope binding energy at a given CE radius $\Delta E_{\rm orb}(a) = E_{\rm env}(a)$, equivalent to $\alpha_{\rm CE} = 1$, (Webbink 1984). The envelope binding energy is computed as

$$E_{\rm env}(a) = \int_{m(a)}^{M} u - \frac{Gm}{r} dm, \tag{13}$$

where we have included both the gravitational binding energy and internal energy of the stellar fluid.

The expression regulating accretion onto the NS is

$$\dot{M}_{\rm NS} = \dot{M}(\epsilon_\rho), \tag{14}$$

where, like the drag, $\dot{M}(\epsilon_\rho)$ is a fit to our numerical results,

$$\log\left(\dot{M}(\epsilon_\rho)/\dot{M}_{\rm HL}\right) \approx m_1 + \frac{m_2}{1 + m_3\epsilon_\rho + m_4\epsilon_\rho^2}, \tag{15}$$

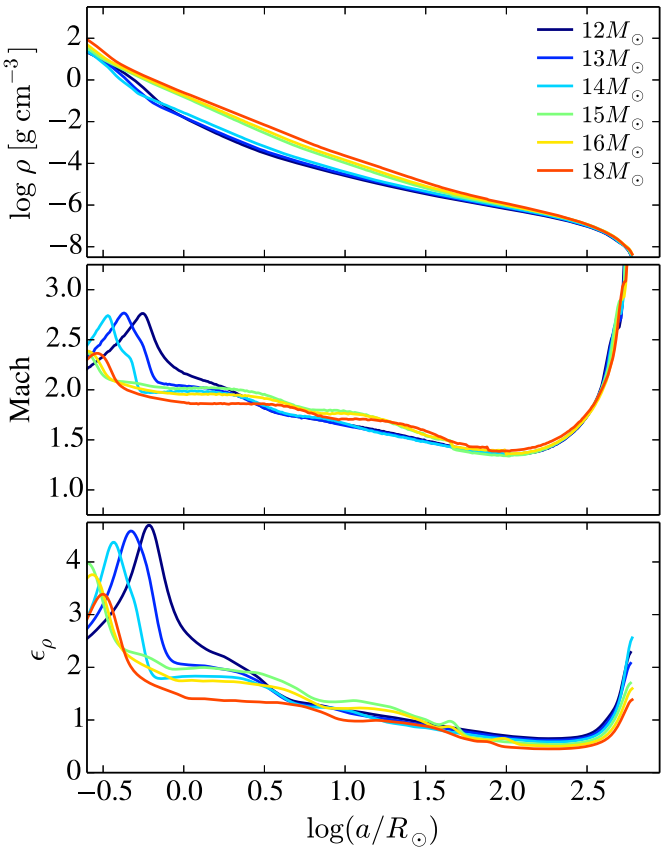

Figure 2. Envelope structure of a range of giant star models that share 600 $R_\odot$. The top panel shows the density profile of the envelopes, while the center and lower panels show flow the Mach number and the density gradient that would be experienced by an inspiralling 1.33 $M_\odot$ NS. For much of the stellar interior, mach numbers are moderate $\mathcal{M}_\infty \approx 1.5$–3 with density gradients of $\epsilon_\rho \approx 1$–2.5, representing substantial density inhomogeneity across the accretion radius. Spikes in the density gradient are seen in the deep interior at transitions in chemical composition.

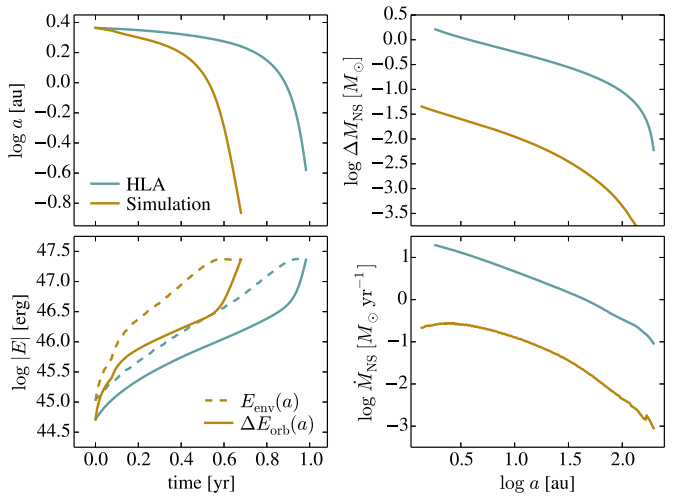

Figure 3. Orbital inspiral of an originally 1.33 $M_\odot$ NS through the envelope of its 12 $M_\odot$, 500 $R_\odot$ companion. The left panels show evolution of the orbital separation (top), and energies (bottom). The right-hand panels show the mass accretion of the NS in terms of the separation. Blue lines show the results assuming HLA, while yellow lines take into account the effect of asymmetry on the accretion rate. In HLA, the NS grows well beyond the maximum NS mass, acquiring more than a solar mass during its inspiral. However, the loss of symmetry in the accretion flow limits $\dot{M}_{\rm NS}$, such that the NS gains less than 0.1 $M_\odot$ and survives the CE.

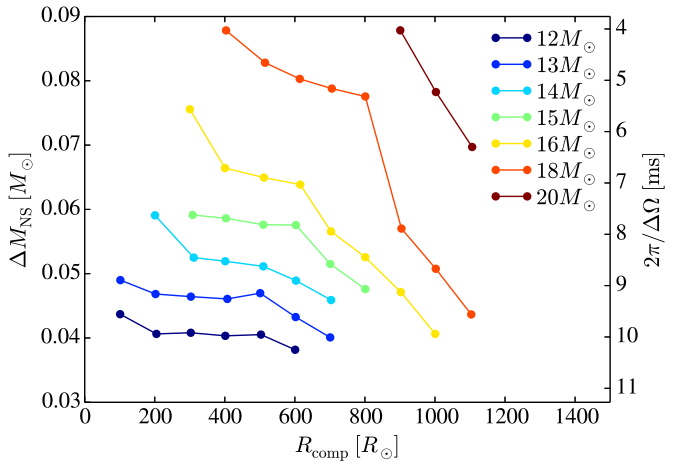

Figure 4. Post-CE states for originally 1.33 $M_\odot$ NSs involved in interactions with wide variety of companions. Companions range in pre-CE mass from 12–20 $M_\odot$, in radius from 100–1100 $R_\odot$, and have convective envelopes. CE events initiated with smaller radius companions than those plotted (for a given mass) result in merger rather than envelope ejection. All evolutions computed result in NSs surviving CE, with none expected to undergo accretion-induced collapse to a BH. NSs generally gain more mass in interactions with more massive companions, but very extended radius at the onset of CE can lead to less mass accumulation. To compute the right-hand axis, we assume material is accreted from a Keplerian disk, and that adopt median NS properties of $M_{\rm NS} \approx 1.39\ M_\odot$, $R_{\rm NS} = 12$ km. NSs undergoing these CE episodes survive to find themselves in close partnerships with helium-rich companions and orbital periods ranging from hours to days.

with $m_i = (-2.14034214, 1.94694764, 1.19007536, 1.05762477)$. To give a baseline for comparison, we also compute orbital inspiral sequences using HLA theory, with $\dot{E}_{\rm orb} = \dot{E}_{\rm HL}$ and $\dot{M}_{\rm NS} = \dot{M}_{\rm HL}$.

We make several approximations that likely lead our calculation of the accreted mass in CE to be an overestimate. First, in assuming a static structure for the CE, we may overestimate the local density of the dispersing envelope (see, e.g., Ricker & Taam 2012). Second, we assume that hypercritical accretion and cooling by neutrinos are effective above $\dot{M}_{\rm hyper}$, despite the fact that this may not apply at all values of $\dot{M} > \dot{M}_{\rm hyper}$, in particular with varying amounts of angular momentum (Fryer et al. 1996; Chevalier 1996; Brown et al. 2000). Finally, we compute the mass accretion rate, Equation (15), assuming that all mass passing through $R_{\rm s} = 0.01\ R_{\rm a}$ is able to propagate the additional two to three orders of magnitude in radial scale to $R_{\rm sh}$, where cooling can occur. Thus, our integration represents an upper limit for the potential accreted mass onto an embedded NS.

3.2. Results

We begin by comparing orbital inspirals based on HLA theory with simulation coefficients for drag and accretion in Figure 3. This comparison highlights the need to consider the role of the structure of the CE around the embedded NS. In the HLA case, the NS gains more than 1 $M_\odot$, enough mass to push it above the $\sim$2 $M_\odot$ maximum NS mass, and in agreement with our analytic prediction of Section 2.1. However, in the simulation case, we see that $\dot{M}_{\rm NS}$ and in turn $\Delta M_{\rm NS}$ are both severely limited by flow asymmetry. $\dot{M}_{\rm NS}$ is still sufficiently high to allow hypercritical accretion to proceed (Chevalier 1993), but the NS gains less than 0.1 $M_\odot$ during its inspiral. This accreted mass represents a few percent of the NS's mass. Thus, the final compact object is a slightly more massive NS, rather than a BH.

We now extend our calculation to consider a diversity of pre-CE structures. In Figure 4, we plot only those structures for which the CE ejection is successful, where $\Delta E_{\rm orb}(a) = E_{\rm env}(a)$ at some radius in the stellar interior. In general, this criteria is satisfied when a distinct helium core and convective envelope structure forms. Minimum orbital periods are in the range 0.1–2 yr as determined by the masses and radii of the companions at the onset of CE. This is in agreement with the analysis of Terman et al. (1995) who found a dividing period of 0.8–2 yr for companions of 12–24 $M_\odot$. CE events involving less-evolved giants (smaller $R_{\rm comp}$ than those plotted) likely lead to complete mergers because the NS is unable to eject its companion's envelope. The merger could result in the formation of either stably burning Thorne–Zytkow objects (Thorne & Zytkow 1977; Levesque et al. 2014) or explosive transients (Fryer et al. 2013).

In each CE structure considered, the NS survives CE. Perhaps more strikingly, it gains only a few percent of its own mass across a broad array of different envelope structures. In general, NSs gain the most mass in interactions with more massive companions. There are two reasons for this effect. First, the NS must spiral deeper to eject its companion's envelope when the mass ratio is larger (Webbink 1984). Second, large mass ratios imply that $R_{\rm a}$ is a smaller fraction of $R_{\rm comp}$, and as a result, the effective density gradient, ϵ_ρ, is reduced (Figure 2), allowing for more efficient accretion (Figure 1). The NS gains less mass in interactions with more extended companions (for a given mass) because these envelopes are comparatively easier to unbind.

Mass accretion implies a spin-up of the NS based on the specific angular momentum of accreting material. In cases where the NS mass is not well determined, the pulsar spin period can still offer constraints on the accreted mass. The spin-up is $\Delta\Omega = \Delta L / I_{\rm NS}$, where ΔL is the accreted angular momentum and $I_{\rm NS}$ is the NS's moment of inertia. We estimate ΔL assuming that material is accreted from a neutrino cooled disk surrounding the NS, $\Delta L \approx \Delta M \sqrt{G M_{\rm NS} R_{\rm NS}}$, and that $I_{\rm NS} = 2/5 M_{\rm NS} R_{\rm NS}^2$. The post-CE spin period of the recycled NS can then be estimated as $2\pi/\Delta\Omega$. The calculated spin periods are shorter than those observed presently for first-born pulsars

in double NS systems ($P \sim 20$–100 ms, Osłowski et al. 2011). However, NSs with magnetic fields $\gtrsim 10^{10}$ G will quickly spin down from these initial periods, so spin constraints are most valuable where the NS magnetic field is small (and thus the spin-down timescale is long). Of the 10 pulsars listed by Osłowski et al. (2011), 2 meet this criterion, pulsars J1518+4904 and J1829+2456. Neither of these object has a well-determined mass, but their measured pulse periods (both ≈ 41 ms) and period derivatives $\lesssim 10^{-19}$ s s^{-1} imply spin down timescales >10 Gyr, allowing direct comparison to Figure 4. If spun-up by accretion during CE, the spin of these objects is consistent with having gained of order 0.01 $M_\odot$.

4. DISCUSSION

We have self-consistently evaluated the mass growth of a NS embedded within a CE, taking into account that the accretion rate depends sensitively on the structure of the CE (MacLeod & Ramirez-Ruiz 2014). Although our integration likely represents an upper limit (as discussed in Section 3.1), we observe that NSs gain only a few percent of their own mass during CE episodes. These objects emerge from CE only mildly heavier and more rapidly spinning, rather than undergoing accretion-induced collapse to BHs (Chevalier 1993; Armitage & Livio 2000). It appears that density gradients in typical CE structures are the missing link needed to reconcile theories of hypercritical accretion onto NSs (Houck & Chevalier 1991; Chevalier 1993; Fryer et al. 1996) with the narrow observed mass distribution of NS masses (Schwab et al. 2010; Özel et al. 2012; Kiziltan et al. 2013). This result hints that forming double NS binaries may not require a finely tuned evolutionary channel (Brown 1995; Bethe & Brown 1998), but they could instead emerge from within the standard CE binary evolution framework (e.g., Stairs 2004; Tauris & van den Heuvel 2006).

Further investigation is certainly needed to probe the efficiency of CE ejection by embedded NSs, as well as the dynamical timescale effects of envelope dispersal (for example, as studied by Terman et al. 1995). We note that a reduction in $\dot{M}$, as compared to $\dot{M}_{\rm HL}$, may hinder envelope ejection in that any potential accretion disk feedback (Armitage & Livio 2000; Papish et al. 2013) would be weakened relative to the envelope's binding energy. This hints that other forms of feedback that may be less dependent on $\dot{M}$, like nuclear burning or recombination, may be of more assistance in CE ejection (Iben & Livio 1993; Ivanova et al. 2014). Studies that consider these energy sources can best determine the critical separation (or orbital period) that divides binaries that merge from those that successfully eject their envelopes.

The CE stage described here is not the full story of the evolution of a binary. In many binaries, the first-born pulsars interact with their helium-star companions following the CE (Tauris & van den Heuvel 2006). If an additional CE were to occur, the low-mass and steep density gradients of the He star's typically radiative envelope (Dewi et al. 2002) suggest a relative ease of envelope ejection and a low accretion efficiency. However, as the most recent interaction, this phase of mass transfer or CE would be responsible for the current spin of the first-born pulsar. These more complex interaction histories are best traced with population synthesis calculations, where the ramifications of observed masses, spins, and orbital eccentricities offer a window to the outcome of the CE phase (Kalogera et al. 2007; Dominik et al. 2012).

We anticipate that moving beyond the energy formalism of CE (Webbink 1984) to also consider CE structure, as parameterized by density gradient ϵ_ρ, will shape the channels through which double compact binaries can be expected to form. As a result of the structures of their companions, few to none of the NSs entering CE episodes should be expected to collapse to BHs.

We thank the anonymous referee for thoughtful and constructive feedback and C. Fryer, J. Guillochon, V. Kalogera, B. Kiziltan, D. Lin, A. Loeb, S. de Mink, R. Narayan, F. Özel, P. Podsiadlowski, M. Rees, T. Tauris, and S. Woosley for guidance and helpful discussions. We acknowledge support from the David and Lucile Packard Foundation, Radcliffe Institute for Advanced Study, NSF grant AST-0847563, and the Chancellor's Dissertation-Year Fellowship at UCSC.

REFERENCES

Armitage, P. J., & Livio, M. 2000, ApJ, 532, 540
Behroozi, P. S., Ramirez-Ruiz, E., & Fryer, C. L. 2014, ApJ, 792, 123
Belczynski, K., Kalogera, V., & Bulik, T. 2002, ApJ, 572, 407
Belczynski, K., Lorimer, D. R., Ridley, J. P., & Curran, S. J. 2010, MNRAS, 407, 1245
Bethe, H. A., & Brown, G. E. 1998, ApJ, 506, 780
Bethe, H. A., Brown, G. E., & Lee, C. H. 2007, PhR, 442, 5
Brown, G. E. 1995, ApJ, 440, 270
Brown, G. E., Lee, C. H., & Bethe, H. A. 2000, ApJ, 541, 918
Chevalier, R. A. 1993, ApJL, 411, L33
Chevalier, R. A. 1996, ApJ, 459, 322
Dewi, J. D. M., Pols, O. R., Savonije, G. J., & van den Heuvel, E. P. J. 2002, MNRAS, 331, 1027
Dominik, M., Belczynski, K., Fryer, C., et al. 2012, ApJ, 759, 52
Fryer, C. L., Belczynski, K., Berger, E., et al. 2013, ApJ, 764, 181
Fryer, C. L., Benz, W., & Herant, M. 1996, ApJ, 460, 801
Fryer, C. L., & Woosley, S. E. 1998, ApJL, 502, L9
Fryxell, B., Olson, K., Ricker, P., et al. 2000, ApJS, 131, 273
Houck, J. C., & Chevalier, R. A. 1991, ApJ, 376, 234
Hoyle, F., & Lyttleton, R. A. 1939, PCPS, 35, 405
Hulse, R. A., & Taylor, J. H. 1975, ApJL, 195, L51
Iben, I. J., & Livio, M. 1993, PASP, 105, 1373
Ivanova, N., Justham, S., Chen, X., et al. 2013, A&ARv, 21, 59
Ivanova, N., Justham, S., & Podsiadlowski, P. 2014, arXiv:1409.3260
Kalogera, V., Belczynski, K., Kim, C., O'Shaughnessy, R., & Willems, B. 2007, PhR, 442, 75
Kiziltan, B., Kottas, A., De Yoreo, M., & Thorsett, S. E. 2013, ApJ, 778, 66
Lee, W. H., & Ramirez-Ruiz, E. 2006, ApJ, 641, 961
Lee, W. H., Ramirez-Ruiz, E., & Page, D. 2005, ApJ, 632, 421
Levesque, E. M., Massey, P., Żytkow, A. N., & Morrell, N. 2014, MNRAS, 443, L94
MacLeod, M., & Ramirez-Ruiz, E. 2014, arXiv:1410.3823
Narayan, R., Paczynski, B., & Piran, T. 1992, ApJL, 395, L83
Narayan, R., Piran, T., & Kumar, P. 2001, ApJ, 557, 949
Osłowski, S., Bulik, T., Gondek-Rosińska, D., & Belczyński, K. 2011, MNRAS, 413, 461
Özel, F., Psaltis, D., Narayan, R., & McClintock, J. E. 2010, ApJ, 725, 1918
Özel, F., Psaltis, D., Narayan, R., & Santos Villarreal, A. 2012, ApJ, 757, 55
Paczynski, B. 1976, in IAU Symp. 73, Structure and Evolution of Close Binary Systems, ed. P. Eggleton, S. Mitton, & J. Whelan (Dordrecht: Reidel), 75
Papish, O., Soker, N., & Bukay, I. 2013, arXiv:1309.3925
Paxton, B., Bildsten, L., Dotter, A., et al. 2011, ApJS, 192, 3
Paxton, B., Cantiello, M., Arras, P., et al. 2013, ApJS, 208, 4
Peters, P. 1964, PhRv, 136, B1224
Phinney, E. S. 1991, ApJL, 380, L17
Popham, R., Woosley, S. E., & Fryer, C. 1999, ApJ, 518, 356
Postnov, K. A., & Yungelson, L. R. 2014, LRR, 17, 3
Ricker, P. M., & Taam, R. E. 2008, ApJL, 672, L41
Ricker, P. M., & Taam, R. E. 2012, ApJ, 746, 74
Schwab, J., Podsiadlowski, P., & Rappaport, S. 2010, ApJ, 719, 722
Stairs, I. H. 2004, Sci, 304, 547
Taam, R. E., Bodenheimer, P., & Ostriker, J. P. 1978, ApJ, 222, 269
Tauris, T. M., & van den Heuvel, E. P. J. 2006, in Compact Stellar X-ray Sources, ed. W. Lewin & M. van der Klis (Cambridge: Cambridge Univ. Press), 623
Terman, J. L., Taam, R. E., & Hernquist, L. 1995, ApJ, 445, 367
Thorne, K. S., & Zytkow, A. N. 1977, ApJ, 212, 832
Webbink, R. F. 1984, ApJ, 277, 355